Metal-oxide-semiconductor photocapacitor for sensing surface plasmon polaritons

Farnood Khalilzade-Rezaie*[a], Robert E. Peale[a], Deep Panjwani[a], Christian W. Smith[a], Janardan Nath [a], Michael Lodge[a], Masa Ishigami[a], Nima Nader[b,c], Shiva Vangala[b,c], Mark Yannuzzi[b], Justin W. Cleary [b]

[a] Department of Physics, University of Central Florida, 4000 Central Florida Blvd, Orlando, FL, USA 32816; [b]Air Force Research Laboratory, Sensors Directorate, Wright-Patterson Air Force Base, OH 45433, USA; [c]Solid State Scientific Corporation, Hollis, NH 0360, U.S.A.

ABSTRACT

An electronic detector of surface plasmon polaritons (SPP) is reported. SPPs optically excited on a metal surface using a prism coupler are detected by using a close-coupled metal-oxide-semiconductor capacitor. Semitransparent metal and graphene gates function similarly. We report the dependence of the photoresponse on substrate carrier type, carrier concentration, and back-contact biasing.

Keywords: Surface plasmon polariton, plasmonics, MOS capacitor

1. INTRODUCTION

Surface plasmon polaritons (SPPs) are electromagnetic waves bound to the surface of a conductor. SPP fields decay exponentially into the dielectric medium above the surface. We recently demonstrated a means of electrically sensing SPPs [1], which were excited on a metal-coated prism surface and detected by a close-coupled graphene/silicon-oxide/silicon photocapacitor. The graphene functioned as a transparent conductor. Biasing the substrate could amplify or extinguish the response. By exploiting the angle- and wavelength-dependent excitation resonances of the prism coupler, the device has potential application as a spectrally-selective photodetector, which could be considered as one pixel in a future compact hyperspectral imager.

Fig. 1(left) presents a device schematic. Electromagnetic radiation is internally incident on a thin metal film on the long face of a Kretchsmann prism coupler [2], where SPPs are excited at a particular frequency determined by the internal incidence angle [2]. We detect them by close-coupling a metal-oxide-semiconductor (MOS) photocapacitor comprising a transparent conductor (TC), a thin layer of SiO_2, and a silicon substrate. Band bending at the Si/oxide interface creates a well that attracts photoinduced minority carriers, whose motion induces a displacement current across the capacitor. DC biasing the blanket back contact, with the top gate contact tied to ground via the internal 50 Ohm input termination of the current preamp, changes the depth of the interface well, amplifying or suppressing the photo current.

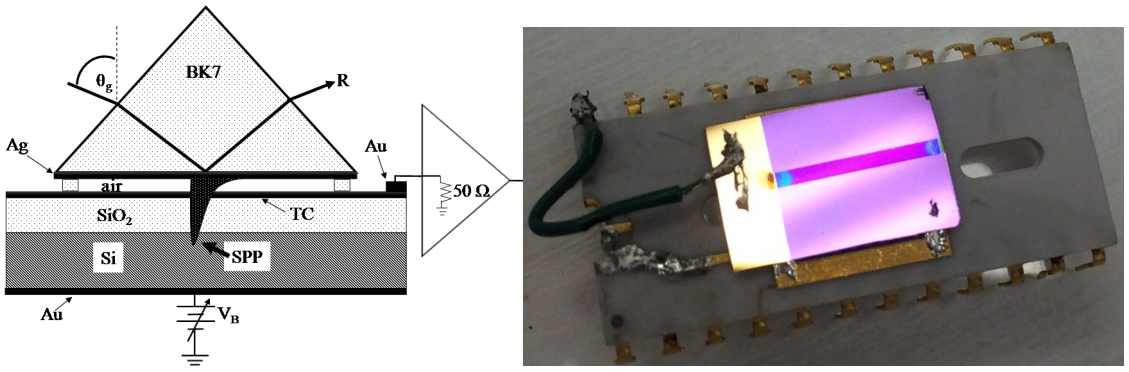

Figure 1 (left) Device schematic. (right) Photograph of MOS photocapacitor mounted on a chip carrier.

*farnood_rezaie@knights.ucf.edu; phone 1 407-823-2325; fax 1 407-823-5112

Unconventional Imaging and Wavefront Sensing 2015, edited by Jean J. Dolne, Thomas J. Karr, Victor L. Gamiz, Proc. of SPIE Vol. 9617, 96170E · © 2015 SPIE
CCC code: 0277-786X/15/$18 · doi: 10.1117/12.2188706

In [1], the TC was graphene. However, the effect is independent of any special properties of graphene besides conduction and transparency. This paper reports a device in which a thin transparent metal serves as the TC. This considerably simplifies the fabrication and reduces sensitivity of the device to static. A first objective of this paper is to demonstrate that with the metal TC similar resonant SPP detection is obtained as with graphene TC. A second objective of this paper is to explore the dependence of the photoresponse on substrate carrier type and concentration. A third objective is to investigate the effect of substrate biasing.

Electronic detection of SPPs has value to future plasmonic devices. Our device is a plasmonic-to-electronic transducer, which will be an essential component of any future plasmonic integrated circuit or sensor. The demonstrated structure suggests application as one pixel in a potential spectral imager. The method is readily extendable to the infrared with proper choice of materials. Thus, the approach is adaptable to a broad range of wavelengths from ultraviolet to mm-waves, depending on the spectral response of the photosensor, the method of exciting the SPP [3], and the conducting film that hosts the SPP [4-9].

2. EXPERIMENTAL DETAILS

Fabrication details for the graphene TC case was described in [1]. Fabrication of the MOS photocapacitor started with a blanket Ti/Au electron-beam evaporated back contact on the unpolished side of a single-side-polished silicon wafer. A blanket layer of SiO_2 on the top polished surface of the wafer was either deposited by plasma-enhanced chemical vapor deposition (PECVD), or it was already present on commercial thermally-oxidized starting wafer. In the latter case, there was also oxide under the back contact. The transparent conducting top contact comprised a 1 mm x 1 cm x 5 nm thick strip of Ti, which was electron-beam evaporated on the oxide through a shadow mask. A 1 cm x 1 cm Ti/Au (50 nm/450 nm) bond pad was deposited on one end of the Ti strip, Fig. 1 (right). The back contact was connected to a Keithley 2400 source meter with current limit set to the 10 nA. The top contact was connected to a Fempto LCA-4K-1G current preamp, whose 50 Ohm internal termination ties the top contact to ground potential in steady state. The preamp and source meter shared a common ground. Connections were made with #30 wire that was indium soldered to the contacts.

For SPP detection experiments, a BK7 right-angle prism was used to excite SPPs on the long face, which was coated with 45 nm of electron-beam evaporated silver. The conducting surface of the prism coupler was mounted facing the TC of the capacitor with an air-gap of 600 nm nominal thickness supported by SiO_2 stand-offs, which were electron-beam evaporated through a shadow mask. The air gap provides the dielectric contrast necessary for SPPs to exist on the silver film. An SPP is represented in Fig. 1 (left) by a decaying intensity distribution that extends into the silicon. A TM-polarized laser of 651 nm wavelength was electrically on-off modulated at 1 kHz. This beam was internally reflected from the metalized prism face while the angle of incidence θ_g was varied by a motor controlled goniometer. Experimental results in this paper are presented in terms of the goniometer angle θ_g indicated in Fig. 1 rather than the angle of incidence internal to the prism. A silicon photodetector rotates at $2\theta_g$ to synchronously monitor the reflected intensity, and the size of the detector element gives an angular uncertainty of about 0.3 deg. Transient charging of the Si/SiO_2 interface induces a displacement current through the capacitor to the current preamp. The voltage output of the preamp was displayed on an oscilloscope, and the transient current was boxcar-integrated and recorded simultaneously with the reflected laser light as a function of θ_g. The laser could be rotated 90 deg to obtain a reference scan in TE polarization.

To study the nature of the photocurrent independently of SPPs, a HeNe laser at 632 nm wavelength passed through a variable set of neutral density (ND) filters, a mechanical chopper at 600 Hz, and finally a lens to focus the beam to a ~100 μm spot on the sample. The output of the preamp was displayed on a digital oscilloscope, which averaged up to 1024 sweeps, and which displayed maximum, minimum, and peak-to-peak voltages that were recorded manually. The chopped incident laser signal was sampled with a beamsplitter and PbSe detector and was displayed simultaneously with the photoresponse, so that the sign of the photocurrent could be determined and recorded. The sign was confirmed by noting the direction of baseline offset due to leakage current when the substrate was biased. Care was taken to avoid saturating the preamp by controlling the laser intensity with the ND filters and by avoiding excessive leakage current as monitored but the current indicated on the source-meter and by the baseline output of the current preamp.

3. RESULTS

Fig. 2 compares SPP resonant photoresponse for photocapacitors with graphene and metal top contacts. For this experiment, an additional 25 nm of Au was deposited on top of the 5 nm Ti strip. It was later noted that the thinner the

metal, the stronger the photoresponse, so that subsequent experiments eliminated the Au overlayer. A peak in the photocurrent occurs close to the angle at which there is a minimum in the reflected light, which is well-known to be associated with generation of SPPs in Kretschmann couplers [2]. A secondary peak occurs at higher angles, and this is due to a back-reflection from the exit facet of the right angle prism. As wavelength decreases, the primary and secondary peaks converge [1], until they coincide at the wavelength where SPP resonance occurs at $\theta_g = 45$ deg, when the beam is normally incident on both entrance and exit facets. TE polarization gives no resonant photoresponse, since SPPs cannot be excited under this condition.

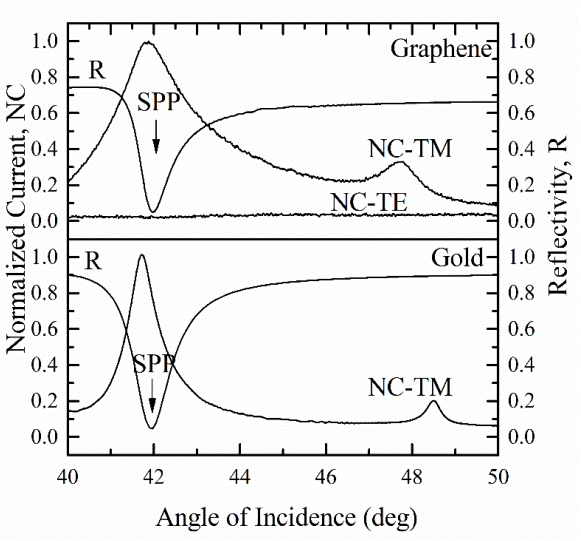

Figure 2. Comparison of SPP resonance detection by photocapacitor with graphene or metal transparent conductor.

Photocurrent peaks in Fig. 2 are slightly shifted to lower angles with respect to the SPP reflection minimum, and there is a small difference in the peak positions for graphene and metal TC devices. The position and width of the primary peaks is very accurately reproduced by Fresnel calculations of transmission into the silicon substrate, considering the thicknesses and complex permittivities of the multiple layers on which the beam is incident. The angular reflectance spectrum is similarly calculated with high accuracy. Thus, the positions and their differences of all peaks in Fig. 2 are as expected by theory. Another notable feature is that the resonances with metal as TC are sharper than they are with graphene, but this can result from small differences in thicknesses, e.g. graphene's thickness of ~2 nm differs significantly from 30 nm Au. Graphene adds essentially nothing to the phase of the wave, while a skin-depth of Au adds ~ 1 wavelength of optical retardation.

To better appreciate the effect of different layer thicknesses, we performed a series Fresnel calculations for transmittance and reflectance. A semi-infinite incident medium of BK7 glass was assumed. A semi-infinite exit medium of silicon was assumed. The photocurrent is proportional to the transmittance into the silicon, since all transmitted light is absorbed there. Prism and TC metal layers were taken as their experimental values and were not varied. Oxide and air-gap thicknesses were varied. Results are presented in Fig. 3. It is already known that strong index contrast on either side of the prism metal is needed to produce a sharp SPP absorption resonance. If there is no air gap at all, there can be no SPP generated. We see that an air gap exceeding 300 nm is needed to produce a sharp resonance. For this calculation we see on resonance that 40% of the incident light is reflected and 30% transmitted, so that 30% is dissipated in the metal without contributing to photocurrent.

When the air gap is as large as 900 nm, the resonance is sharp, but the silicon is so far down in the tail of the evanescent SPP fields that the transmittance (and photocurrent) are small. At the peak, reflectance is ~0% and transmittance is 30%, so that 70% of the incident light is dissipated in the metal.

The optimum air gap appears to be 600 nm, which corresponds to the experimental situation. Proximity of dielectric to the prism enhances transmission, as in frustrated total internal reflection. If the oxide is thick, the resonance is broad, but only 16% is dissipated in the metal. The thinner oxide brings the higher index silicon closer to the SPP, increasing the transmittance, and interestingly the resonance also sharpens. Then, peak T and R are 50 and 0%, respectively, so that half the incident light is dissipated in the metal.

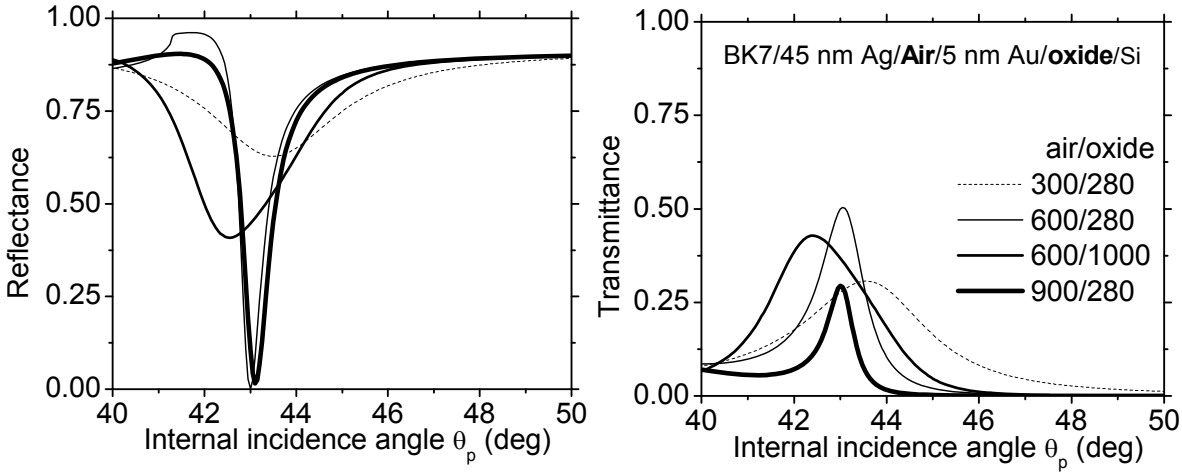

Figure 3 Fresnel calculations of angular reflectance and transmittance spectra with varied air gap and oxide thicknesses (given in nm).

Fig. 4 presents the results of calculations for various air gaps and oxide thicknesses. Results show that the peak transmittance oscillates between about 30 and 50%, with the phase of the oscillation depending on the air-gap thickness. Additional calculations for single value of the air gap show that between 280 and 1000 nm of oxide there is little dependence of T_{max} on oxide thickness. In other words, once the SPP fields have crossed the air gap and entered the oxide, they are transmitted into the silicon, regardless of the oxide's thickness. The small oscillatory variations with oxide thickness are not surprising, because the multi-layer structure consists of multiple Fabry-Perot cavities. Quantitative analysis of those oscillations will require calculations over a broader range of thicknesses in smaller thickness steps.

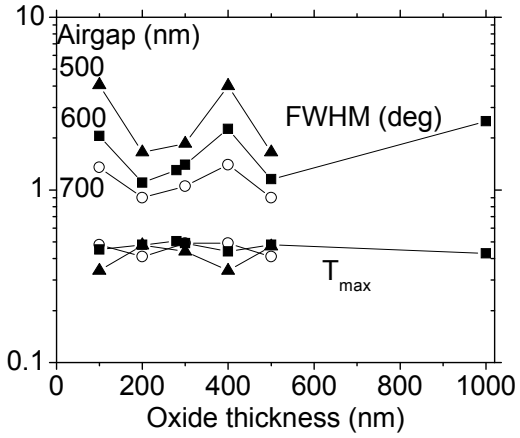

Figure 4. Peak transmittance into silicon and resonance full width at half maximum as a function of MOS oxide thickness for various air gaps between SPP prism coupler and MOS photocapacitor.

The resonance full-width at half maximum is a much stronger function of both air gap and oxide thickness. The resonances sharpens monotonically with increasing air gap for given oxide thickness, and it oscillates strongly with oxide thickness for given air gap thickness. Here, the phase of the oscillations is independent of oxide thickness. For spectrally selective applications, a sharp resonance is desired, so investigation of these effects at over a broader range of thicknesses at smaller thickness steps will be important.

In the graphene-based device, we previously noted that a photocurrent appeared when the silicon substrate was p-type of moderate resistivity in the range 10-25 Ω-cm, but not in more heavily-doped p-Si. We next investigate the nature of the photocurrent and its dependence on substrate doping level and type. These experiments were performed without the prism and no attention to polarization. Fig. 5 presents oscilloscope traces for two samples that differ mainly in substrate doping type. Secondary differences are that the oxide on the p-Si device is PECVD with thickness 280 nm, while the oxide on

the n-Si device is thermally grown with thickness 1 μm. We see that when the chopper admits the light onto the Ti stripe, there is a positive transient photo-current in the case of n-Si, while for p-type, the photocurrent is negative. Both samples had similar manufacturer specified resisitivities (1-10 and 1-20 Ω-cm, respectively). When the chopper blocks the beam, capacitor discharge currents are observed of opposite sign to the photocurrent, whose sign is consistent with flow of photo-induced minority carriers toward the substrate/oxide interface. The strength of the photoresponse can be varied by changing the ND filters or by applied substrate bias, as shown below. For the same conditions, the signal from the p-Si sample was much stronger, which we attribute to its thinner oxide. There was no photoresponse observed at all for a sample with heavily doped p-Si substrate (1-5 mΩ-cm, 280 nm PECVD oxide) or for a sample with heavily doped n-Si substrate (6.7 mΩ-cm, 300 nm thermal oxide). There was a weak negative photocurrent observed for undoped p-Si (3 kΩ-cm, 280 nm PECVD oxide).

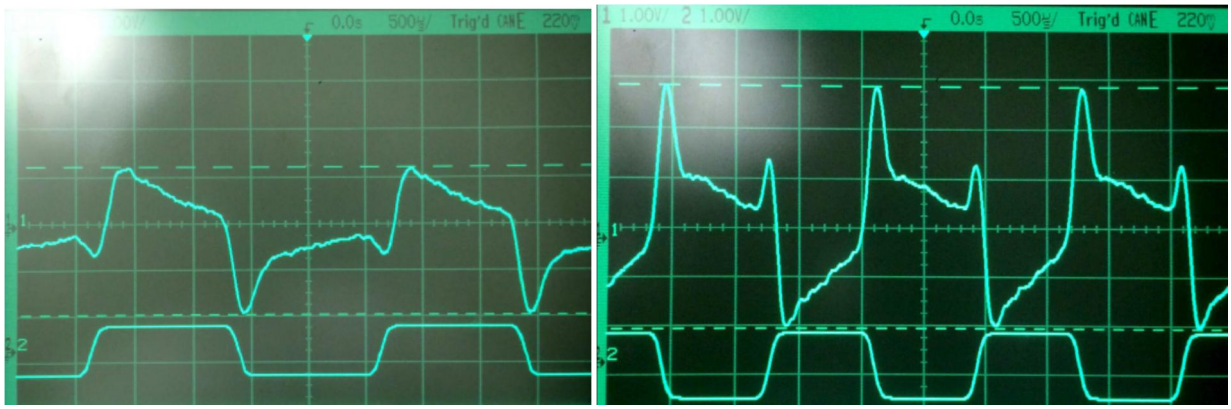

Figure 5. Oscilloscope traces of photocapacitor current (upper) and incident laser intensity (lower) for p-type (left) and n-type (right) substrates. The output of the PbSe detector amplifier is inverting, so that low voltage corresponds to "laser on".

When 25 nm of Au was added to the Ti stripe, the photo response was weak when the laser was centered on the stripe, due to reduced transparency. For such samples, displacing the laser to the side of the stripe generated a photocurrent of the opposite sign, i.e. positive for p-type substrates. The magnitude of this "side" photocurrent was nearly independent of the position of the laser spot beyond about 0.1 mm from the edge of the metal. We attribute this photocurrent to local trapping of photogenerated minority carriers at the semiconductor/oxide interface and displacement of the background majority carriers by the photogenerated majority carriers toward the contacts. When the strip was just 5 nm thick Ti, this oppositely-signed "side" current was not observed. Fig. 6 presents a plot of normalized photocurrent versus laser spot position as it is translated across a 5-nm-thick 1-mm-wide Ti strip, with the zero of position scale corresponding to the center of the strip. There is signal within the 1 mm strip, but there is none outside. Photocurrent is positive for n-type substrate and negative for p-type.

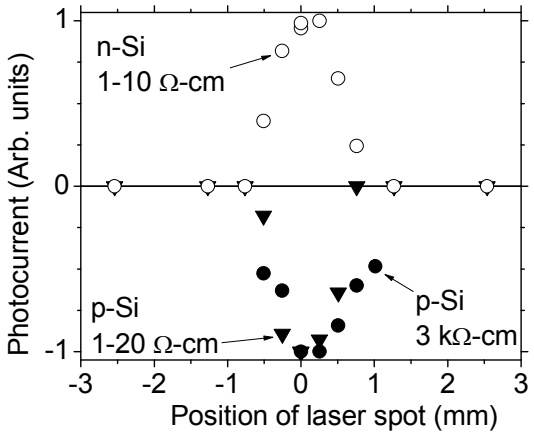

Fig. 6. Normalized amplitude of transient photocurrent from MOS photocapacitor for two p-type substrates (1-20 and 3000 Ω-cm, 280 nm PECVD oxide) and one n-type substrate (1-10 Ω-cm, 1 μm thermal oxide) as a function of position for the focused HeNe laser on the 1-mm-wide 5-nm-thick Ti strip.

Fig. 7 presents the effect of biasing the substrate. We see that a positive bias increases the photoresponse for the n-type device and decreases it for the p-type device, and vice versa. Much larger biases can be applied to the n-type device because its thick thermal oxide is less prone to leakage current, which we do not allow to exceed a few nA. Sufficient negative bias could be applied to the n-type device to extinguish the photoresponse entirely. In the MOS devices, the bias effect is fairly flat and linear at low bias values, but it becomes steep and linear for high biases. This behavior differs from that for the graphene device, where the effect is steep (shallow) at low (high) bias [1].

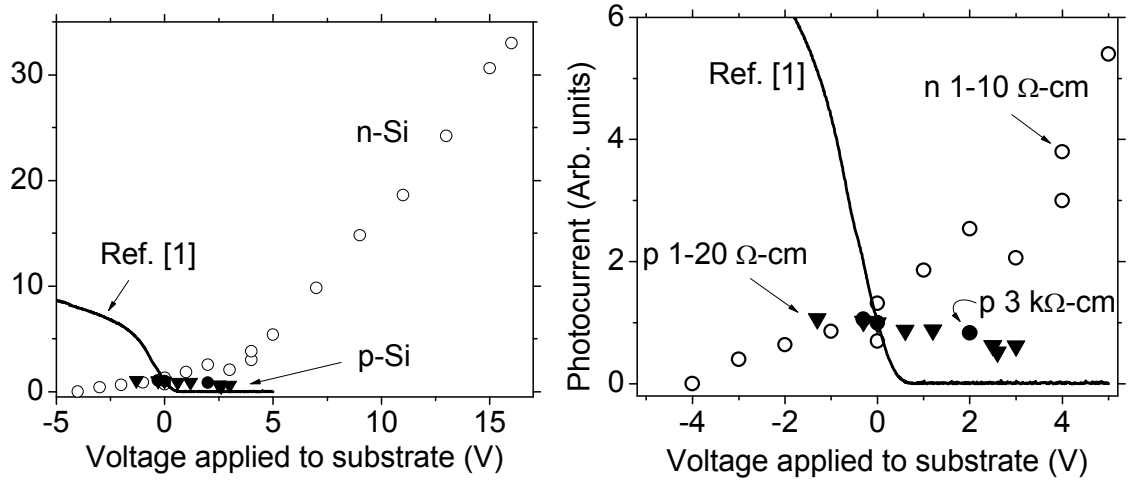

Figure 7. Magnitude of photocurrent as a function of back-contact bias. All data are normalized to unity at zero bias. (left) Wide bias range. (right) Close-up of behavior near zero bias. Data the graphene device [1] is included for comparison.

4. DISCUSSION

The signs of the photocurrents in Figs. 5 and 6 are consistent with photogenerated minority carriers traveling toward the silicon/oxide interface, inducing a transient displacement current through the capacitor, which is amplified by the preamp. Back-contact bias of the same sign as that of the minority carriers drives them toward the interface, increasing the magnitude of the transient current, which explains the observations in Fig. 7.

An important difference between the graphene device presented in [1] and Ti devices reported here is how the bias was applied. In the graphene device, the contact to the substrate was placed at a point *on top* of the substrate through an opening in the oxide. Additionally, one side of the graphene strip was grounded, but because the graphene's total resistance was 22 kΩ, the center of the strip was tied to ground by the relatively large resistance of ~11 kΩ. The other end of the

strip was tied to ground via the input impedance of the preamp, as in the experiments reported here. In contrast, the Ti devices studied here had bias applied uniformly over a backside blanket contact, and the relatively low resistance of the Ti strip made it an equipotential. As long as there is no photocurrent in the substrate, where the bias is applied is immaterial since the semiconductor would be a constant potential in steady state. But when non-steady-state photocurrent is present, the semiconductor is not at an equipotential, and the geometry of the bias contact can affect the flow of current toward the preamp. These differences indicate that bias contact geometry is a potentially useful variable for optimizing the device performance.

We have identified that the observed photocurrent is a transient displacement current through a metal-oxide-semiconductor (MOS) photocapacitor. The current is caused by migration of photogenerated minority carriers toward the silicon/SiO_2 interface. We noted that the magnitude of this current is zero when the substrate resistivity is very low and small when the resistivity is very high. We interpret the dependence on resistivity as follows. For photogenerated minority carriers to be drawn toward the said interface, these carriers must be generated within the region where there is band bending. This is the depletion region, whose width reaches a maximum value W_T at the threshold between depletion and inversion. For 0.005 Ω-cm, W_T is a few nanometers [10], which is much less than the ~1 μm absorption depth for above gap radiation in Si [11], so that for such substrate the most of the photo-generated minority carriers feel no attraction to the interface. On the other hand, for 3000 Ω-cm substrate, $W_T \sim 10$ μm, and there must be a different reason for the small photocurrent observed. We suggest that the photocurrent is inversely proportional to capacitive reactance, i.e. it is proportional to capacitance, and this is smaller the larger that W_T becomes. Thus, we expect the maximum photocurrent to occur for substrates with intermediate resistivity, which supports our observation of strong photocurrent only when MOS structures were fabricated on n- or p-type substrates with 1-20 Ω-cm resistivity. Interestingly, for such intermediate resistivity, W_T is approximately the same as the absorption depth and capacitance is approximately half the maximum possible value, which occurs when the MOS structure is in accumulation.

5. SUMMARY

An MOS-based detector of surface plasmon polaritons (SPP) was investigated. Dependence of the response on substrate carrier type, carrier concentration, and back-contact biasing was reported. Layer thicknesses were theoretically optimized to achieve the strongest and angularly-sharpest resonant response to SPPs excited on a prism coupler.

ACKNOWLEDGMENTS

FKR acknowledges support from University of Central Florida's research excellence fellowship and Northrop-Grumman scholarship. Work by UCF authors was partly supported by Florida High Technology (I-4) program. JWC and NN were supported by Air Force Office of Scientific Research under AFOSR LRIR No. 12RY10COR (Program Officer Dr. Gernot Pomrenke). REP was partially supported by the AFRL Sensors Directorate. CSW, ML, and MI were supported by the National Science Foundation under Grant No. 0955625.

REFERENCES

[1] Smith, C.W., Maukonen, D., Peale, R. E., Fredricksen, C. J., Ishigami, M., and Cleary, J. W., "Wavelength-selective visible-light detector based on integrated graphene transistor and surface plasmon coupler," Proc. SPIE 9083-102 (2014).

[2] Kretschmann, E., "Die Bestimmung optischer Konstanten von Metallen durch Anregung von Oberflaechenplasmaschwingungen," Z. Physik 241, 313 (1971).

[3] Cleary, J. W., Medhi, G., Peale, R. E., and Buchwald, W. R., "Long-wave infrared surface plasmon grating coupler," Applied Optics 49, 3102 (2010).

[4] Cleary, J. W., Peale, R. E, Shelton, D. J., Boreman, G. D., Smith, C. W., Ishigami, M., Soref, R., Drehman, A., and Buchwald, W. R., "IR permittivities for silicides and doped silicon," JOSA B 27, 730 (2010).

[5] Cleary, J. W., Medhi, G., Shahzad, M., Rezadad, I., Maukonen, D., Peale, R. E., Boreman, G. D., Wentzell, S., and Buchwald, W. R.,"Infrared surface polaritons on antimony," Optics Express 20, 2693, (2012).

[6] Shahzad, M., Medhi, G., Peale, R. E., Buchwald, W. R., Cleary, J. W., Soref, R., Boreman, G. D., and Edwards, O.,"Infrared surface plasmons on heavily-doped silicon," J. Applied Physics 11, 123105 (2011).
[7] Khalilzadeh-Rezaie, F., Smith, C. W., Nath, J., Nader, N., Shahzad, M., Cleary, J. W., Avrutsky, I., and Peale, R. E., "Infrared surface polaritons on bismuth," J. Nanophotonics 9, 093792 (2015).
[8] Cleary, J. W., Streyer, W. H., Nader, N., Vangala, S., Avrutsky. I., Claflin, B., Hendrickson, J., Wasserman, D., Peale, R. E., and Buchwald, W. R., "Platinum germanides for mid- and long-wave infrared plasmonics," Optics Express 23, 3316 (2015).
[9] Khalilzadeh-Rezaie, F., Oladeji, I. O., Cleary, J. W., Nader, N., Nath, J., Rezadad, I., and Peale, R. E., "Fluorine-doped tin oxides for mid-infrared plasmonics," Optical Materials Express, submitted (2015).
[10] Pierret, R. F., Semiconductor device fundamentals, Addison-Wesley (1996).
[11] Wooten, F., Optical properties of solids, Academic press (2013).